SAE International

2012-01-0171
Published 04/16/2012

doi:10.4271/2012-01-0171
saepcmech.saejournals.org

Bluff Body Drag Reduction with Ventilated Base Cavities

Jeff Howell
Tata Motors European Technical Centre

David Sims-Williams, Adam Sprot, Fred Hamlin and Robert Dominy
Durham University

ABSTRACT

Various techniques to reduce the aerodynamic drag of bluff bodies through the mechanism of base pressure recovery have been investigated. These include, for example, boat-tailing, base cavities and base bleed. In this study an Ahmed body in squareback configuration is modified to include a base cavity of variable depth, which can be ventilated by slots. The investigation is conducted in freestream and in ground proximity. It is shown that, with a plain cavity, the overall body drag is reduced for a wide range of cavity depths, but a distinct minimum drag condition is obtained. On adding ventilation slots a comparable drag reduction is achieved but at a greatly reduced cavity depth. Pressure data in the cavity is used to determine the base drag component and shows that the device drag component is significant. Modifications of the slot geometry to reduce this drag component and the effects of slot distribution are investigated. Some flow visualisation using PIV for different cavity configurations is also presented.

CITATION: Howell, J., Sims-Williams, D., Sprot, A., Hamlin, F. et al., "Bluff Body Drag Reduction with Ventilated Base Cavities," *SAE Int. J. Passeng. Cars - Mech. Syst.* 5(1):2012, doi:10.4271/2012-01-0171.

INTRODUCTION

Aerodynamic drag of a typical passenger car arises from a near equal split between the styled upper surfaces and the less visible components comprising; cooling airflow, underbody, wheels and wheelarches. On the upper surfaces the major drag component, 60%, occurs at the rear of the car, and dominates the drag from the front end, skin friction and protuberences such as mirrors. This constitutes approximately 30% of the overall aerodynamic drag and it results from the suction which occurs on the rearward facing surfaces, especially those in the separated flow regions at the base of the car. Similarly, from the less visible components, the wheels and wheelarches contribute approximately 30% of the overall aerodynamic drag. Any investigation into drag reduction must concentrate on these significant contributors.

Improving the rear end drag must primarily concentrate on increasing the pressure on the base and comes under the general heading of 'base pressure recovery'. The main routes for achieving this are, rear body tapering (boat-tailing), base cavities and base flow injection. Boat-tailing effects can be seen in saloon and fastback car shapes, and although the top surface tapering for these vehicles tends to be excessive, rear bodyside tapering contributes to an increase in base pressure. It has also been exploited on 1- and 2-box shapes through the combined effects of roof and bodyside curvature, although design constraints have limited these benefits. Significant drag reduction has been demonstrated on trucks with the use of angled base boards to provide a combination of cavity with boat-tailing effects, as exemplified by Cooper (1) and Browand et al (2). Very few experiments on base flow injection, applicable to road vehicle type bodies, have been reported. Exceptions are the work of Englar (3), with high velocity Coanda type jets, and Sykes (4) and Howell et al (5) using low velocity bleed flow. Interestingly, the latter study showed that a significant part of the drag reduction achieved came from the cavity

While a significant amount of research has been conducted on the effect of base cavities on drag reduction for axisymmetric bodies at high Mach numbers relevant to missile aerodynamics, as shown, for example, in the comprehensive review by Viswanath (6), very few studies have been at the low subsonic Mach numbers relevant for automobiles. Exception are Morel, (7), who tested a slender axisymmetric shape of small diameter in freestream and Duell, (8,9), who investigated a small model of square section near to a ground plane. Morel showed that useful drag reduction was obtained with a simple cavity, but also that ventilating that cavity produced a similar benefit but at a reduced cavity depth.

In addition to the truck cases cited earlier, Mason and Beebe (10) reported on the application of a plain cavity to a truck model, while Hucho (11) includes a reference to tests with a plain cavity added to the rear of a light van. Both showed useful drag benefits, but more recently Irving Brown et al (12) investigated base cavities on an SUV and found the drag reduction was insignificant.

To explore the potential for drag reduction from base cavities it was decided to conduct a similar study to that of Morel, but using a larger model, more representative of a car shape, with a rectangular cross section. The cavity would be plain and ventilated, of variable depth and the body would be tested both in freestream conditions and in ground effect.

EXPERIMENTAL STUDY

MODEL

The model used was a copy of the Ahmed body, (13). It was originally made by Rover, many years ago, as a reference body and was of wooden construction. The overall model dimensions were: length 1.044m, width 0.389m, height 0.288m. The leading edge radius is 0.10m. The model was modified by removing some internal structure at the rear to facilitate a plain cavity, and the removeable upper body sections were replaced with a fixed squareback shape with an open base. A sliding back-plate for the cavity, which could be positioned from outside the model, gave a maximum cavity depth of 0.25m. The cavity walls were 0.012m thick and longitudinal ventilation slots were cut into the walls. The model and the slot arrangement are shown in Figure 1.

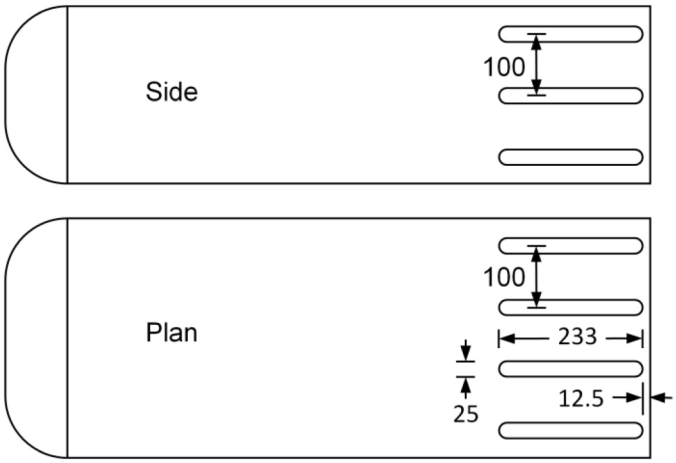

Figure 1. Ahmed body showing cavity ventilation slot dimensions (mm).

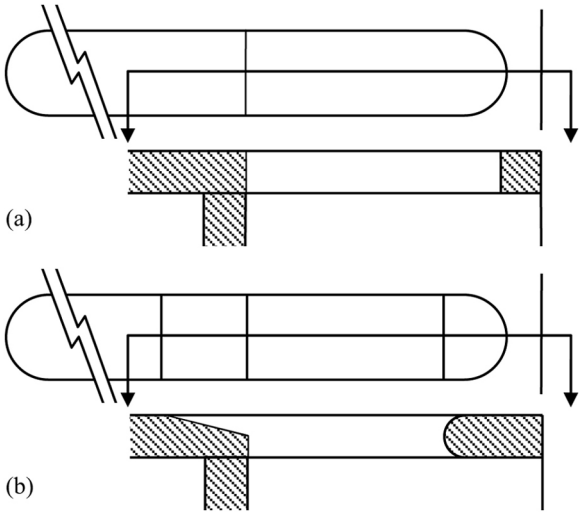

Figure 2. Ventilation slot details (a) Square edged, (b) Tapered.

The 14 slots were uniformly spaced at 0.10m and were cut into the top, bottom and side body surfaces. Each slot was 0.233m long and 0.025m wide. The slot ends were semicircular and the distance between the slot end and the body trailing edge was 0.0125m. For cavity depths less than the maximum slot length the forward section of the slot was filled and the slot leading edge shape was squared off. A section through the slot is shown in Figure 2(a), and is here called a square edged slot. A subsequent modification to try and reduce the drag due to the slot, known as the device drag, following Viswanath (6), and which is here called a tapered slot is shown in Figure 2(b).

WIND TUNNEL

The wind tunnel used in this experiment is a low speed, open jet, straight through wind tunnel in the School of Engineering and Computing Sciences at Durham University. It has a nozzle 1.75m wide by 1.15m high and the working section is 5m long. The normal operating speed of the tunnel is 25m/s. The wind tunnel can be operated with a moving belt or a solid floor for ground simulation, but for all tests conducted here the tunnel was operated with a fixed ground. The model was mounted to an under floor 6-component balance, which could be yawed. Total repeatability for the facility is ±0.002 for drag coefficient and multiple repeats of the baseline configuration were within that range. Further details of the facility are available in (14), (15).

The model is shown in the wind tunnel in Figure 3 with tapered ventilation slots. The slots on the lower wall of the cavity are, in this case, filled. In ground proximity the model was mounted on cylindrical legs, diameter 0.025m, and the ground clearance was set at 0.060m. Wind tunnel blockage was 5.6% and the forces were corrected for blockage according to SAE SP 1465, (16). In nominally freestream conditions the model was mounted on elongated legs which positioned the model centrally relative to the nozzle.

The nominal freestream wind velocity was 25m/s in all cases except where the effect of Reynold's Number was investigated. The nominal test speed gave Re = 1.80×10^6 based on model length. Drag coefficient showed a small consistent reduction with increasing Reynold's Number. For all configurations increasing Re from 1.08 to 1.8×10^6 produced a drag coefficient reduction in the range of ΔC_D =0.010−0.014, which represents approximately 3-4% of the total drag for the squareback model without a cavity.

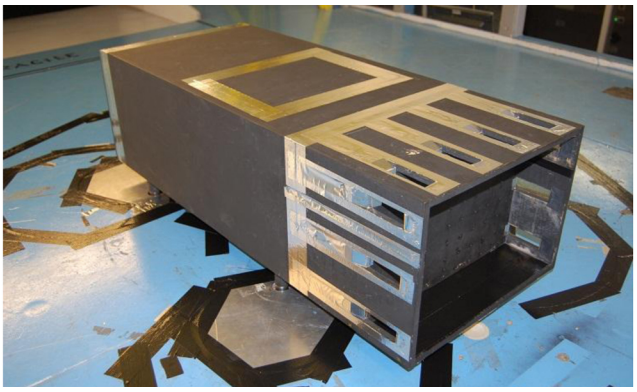

Figure 3. Ahmed body with ventilated cavity in the Durham University Wind Tunnel

PARTICLE IMAGE VELOCIMETRY (PIV)

PIV was used in the longitudinal orientation (x-y plane) on the model centerline at three different cavity depths. The system comprised a pulsed 120mJ dual head Nd:YAG laser, which was placed 2.2m downstream of the model trailing edge. Two cameras (12 Bit Sensicam 1280×1024 with chip cooling) were used to take simultaneous instantaneous flow fields. The image field of each camera was 0.18m wide by 0.20m high and the cameras were traversed to three locations downstream of the model base, where the six fields were stitched together electronically to create the final flow field maps. The flow was seeded using DEHS oil distributed by a compressed air fed atomizer, which produced consistent particles of around 1µm diameter. These were fed into the flow upstream of the nozzle contraction via a purpose built smoke delivery rake. The system was synchronised electronically and the pulse separation was set to 15 µ.S. This allowed adequate particle separation between images to pick up fine resolution of velocities but was also small enough to prevent drop-out, where a particle from the first image is no longer present in the image field of the second exposure. Each interrogation involved 200 image pairs, which were selectively averaged to include only valid vectors.

5-HOLE PRESSURE PROBE

Additional flow field data were obtained using a 5-hole probe. The probe has a head dimension of 3mm and comprises a stainless steel body with a rapid-prototyped acrylic head which can be replaced if damaged in service. The probe was calibrated to provide a pitch and yaw range extending to ±60°. The focus of the present work was on time-averaged measurements and so no time-resolved calibrations were performed but the probe nevertheless provides some information about levels of unsteadiness, characterized by the level of pressure fluctuation seen at the centre hole.

RESULTS

The initial tests of the modified Ahmed model were conducted out of ground effect. The effect of a cavity depth for a plain cavity, ie with no ventilation slots, is shown in Figure 4. The incremental drag coefficient is measured relative to the standard Ahmed body in squareback configuration with no cavity. In this test the baseline drag coefficient, C_D, was 0.339, although it should be noted this included a substantial tare drag correction for the elongated support struts. As cavity depth increases, drag is initially reduced rapidly, but then levels off with a minimum drag coefficient at a cavity depth of 0.140m.

Adding the ventilation slots, the drag reduction due to cavity depth is initially similar to the solid walled cavity, but at a cavity depth of 0.060m the minimum drag is achieved and at greater depths the drag increases rapidly. At a cavity depth of 0.125 m the drag becomes equal to that of the basic body. The vented cavity shows no improvement over the plain cavity.

The central slot on the side and the two middle slots on the top and bottom surfaces of the body were taped over to investigate crudely the effect of ventilation area on the drag. The minimum drag was the same as that obtained with the full set of ventilation slots. The penalties arising from the slots at cavity depths greater than the optimum could, however, be mitigated by reducing the ventilation area. This suggests that the slots are a source of drag.

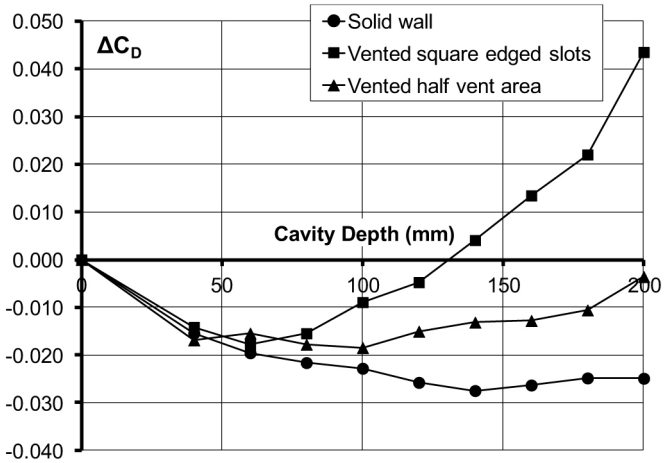

Figure 4. Effect of cavity depth for body in 'freestream'.

The body was then set up close to the ground with a ground clearance of 0.060m and the effects of cavity depth on

drag determined for the plain and ventilated cavity. The effect on drag is shown in Figure 5, relative to the squareback configuration, (C_D = 0.328). The plain cavity shows a reduction in drag coefficient with cavity depth which is very similar to the 'freestream' case, and the drag minimum occurs at a cavity depth of 0.130m. The maximum drag reduction obtained with the ventilated cavity, however, was the same as in the freestream condition, but the minimum drag coefficient occurred with a cavity depth of 0.10m, which was deeper than the 'freestream' case. The drag rise as cavity depth increased further was considerably slower than for the freestream case.

A modification to the slot geometry was made in an attempt to reduce the component of drag due to the slots themselves, which Viwanath, (6) has called the device drag. This was obtained with a ramp on the front edge of the slot, leading into the cavity, and a radius on the rear edge of the slot and is designated as a vented tapered slot. These changes resulted in a small reduction to slot area, as shown in Figure 2(b). The effect on drag is plotted in Figure 5. No short cavities were tested but the drag minimum occurs at a reduced cavity depth of approximately 0.08m, and a steep drag rise is seen for deeper cavities. Some sensitivity to cavity depth is apparent as a drag 'bucket' occurs around the minimum drag condition. The drag benefits from the cavity in this region are greater than for the vented cavity, but do not exceed that for the plain cavity.

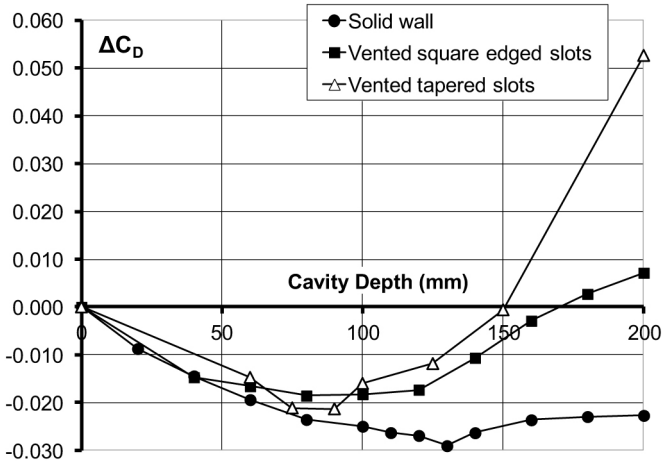

Figure 5. Effect of cavity depth for body near to ground.

An additional test was conducted to assess the effect of changing individual walls, and combinations of walls, of the cavity from ventilated to plain. This was done for a fixed cavity depth of 0.075m and the ventilated slots incorporated the tapered modification. The results are shown in Figure 6. In all cases, except one, the ventilated slots produced higher drag than the plain cavity. When the bottom surface of the cavity was sealed, however, a significant drag reduction over the plain cavity was observed. In this configuration the effect of cavity depth on drag coefficient was investigated. The result is shown in Figure 7. In comparison with the body having all the cavity walls slotted the drag is reduced throughout the range of cavity depth. The reduction is marked around the minimum drag condition, which occurs for a cavity depth of approximately 0.090m. The drag minimum is also slightly less than that for the plain cavity.

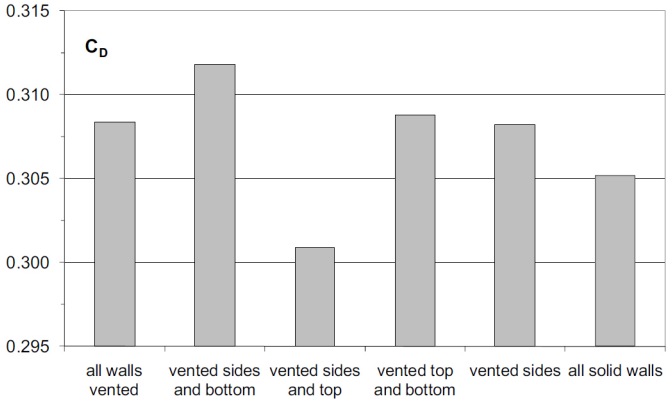

Figure 6. Effect of venting individual cavity walls.

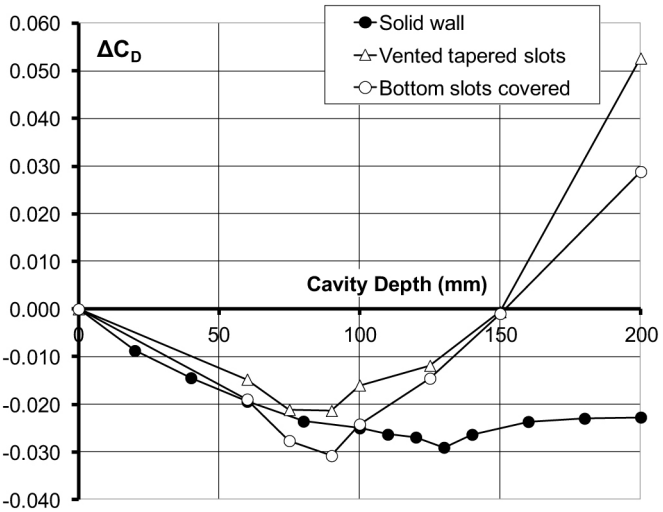

Figure 7. Effect of cavity depth for body with bottom slots covered.

ANALYSIS

For the body with a plain cavity in freestream the maximum reduction in drag coefficient, $\Delta C_D = -0.028$, relative to the squareback configuration, is obtained at a cavity depth of 0.140m. This is a very similar improvement in drag to that found by Morel (7) for a small scale axisymmetric body, $\Delta C_D = -0.029$. Non-dimensionalising the optimum cavity depth, L, with respect to the equivalent diameter, D_e, where the frontal area, $A = \pi D_e^2/4$, gives $L/D_e = 0.371$. This compares with $L/D_e = 0.36$ for the body tested by Morel, (7). Morel also showed that the base pressure coefficient increased with cavity depth up to the minimum drag condition and thereafter remained constant. Viswanath

(6) investigated the effect of cavity depth on drag of another axisymmetric body at transonic speeds. At the minimum Mach number, M, of 0.7 it was concluded that the minimum drag occurred at a cavity depth greater than 0.4 × the body diameter. The drag reduction from the cavity also increased with Mach number, but at M=0.7 was only a third of that found in the low speed tests. Viswanath also showed that an optimum wall thickness, t, for the cavity could be defined at approximately t/D_e =0.075. The Ahmed body, reported here, and the Morel body had cavity wall thicknesses of t/D_e =0.033 and 0.026, respectively.

Adding ventilation slots to the Ahmed body in freestream, in the experiment reported here, produced a minimum drag coefficient at a considerably reduced cavity depth, L/D_e = 0.159 in comparison with the plain cavity. However the reduction in the overall drag coefficient was also reduced at $\Delta C_D = -0.018$. Morel (7) had shown that the maximum drag reduction for the ventilated cavity on an axismmetric body was identical to that for the plain cavity and it occurred at a cavity depth of L/D_e =0.20. Both studies show that for cavities deeper than optimum the drag coefficient increases rapidly. It has been shown in this experiment that this drag rise is reduced considerably if the ventilation area is reduced, with no change to the drag benefit. The ventilation area ratio, A_v, (defined crudely by the slot width times the number of slots as a function of the body circumference, for the Ahmed body tested here and the Morel study are comparable at A_v = 0.26 and 0.32 respectively.

With the body in ground proximity, z_0/D_e = 0.178, where z_0 is the ground clearance, there are no dramatic differences in the performance of the plain cavity. The maximum drag reduction is increased slightly to $\Delta C_D = -0.029$ and it occurs at a cavity depth of 0.130m, L/D_e = 0.345. Howell et al (5) while investigating base bleed on the Windsor body, with an identical rear cross section, also studied a plain cavity with and without a porous base. Ground clearance was z_0/D_e = 0.133. The maximum drag reduction was comparable to that found in this experiment, $\Delta C_D = -0.031$ but was obtained with a cavity 0.100m deep, L/D_e = 0.265. The addition of a porous base did not significantly alter the cavity depth for minimum drag but the drag benefit was reduced. Duell and George (8) also investigated the effect of cavity depth on a square section body in close ground proximity where z_0/D_e = 0.071. No drag measurements were reported but the base pressure was shown to be still increasing at a cavity depth of L/D_e = 0.71. It could, however, be interpreted that the base pressure increase was negligible for cavities deeper than half this, and may indicate a drag minimum close to L/D_e = 0.35.

For the ventilated cavity on the Ahmed body in ground proximity the maximum drag reduction is the same as that found in freestream, $\Delta C_D = -0.018$, but it occurs for a cavity depth of L/D_e = 0.237, slightly greater than the depth for the body in freestream. The subsequent drag rise with cavity depth is, however, considerably reduced. It was felt that a considerable drag penalty was arising from the effects of the ventilation slots, themselves. In an attempt to reduce this so-called 'device drag' component the slot geometry was modified as shown in Figure 2(b). The front edge of the slot was changed from a square edge to a ramp and the rear edge was rounded using inserts. The result, denoted by 'vented tapered slot' is seen in Figure 5 to be negative for most of the cavity depth range but for a very narrow range of cavity depth the modification shows an increased drag reduction in comparison with the ventilated cavity.

A drag 'bucket' occurs for cavity depths between 0.075m and 0.09m, L/D_e = 0.223−0.267, but the drag reduction of $\Delta C_D = -0.022$ still does not match that of the plain cavity. The drag rise at greater cavity depths is as large as that for the ventilated cavity in freestream. The only configuration tested, which produced a drag reduction greater than that of the plain cavity, was with the slots on the underside of the cavity sealed up, as shown in Figure 7. The remaining slots were all faired and as for the configuration with all the faired slots open a drag 'bucket' is also apparent for the same range of cavity depths, L/D_e =0.223−0.267, with a maximum drag reduction of ΔC_D =−0.032 at L/D_e =0.267. The existence of a distinct drag bucket could suggest that the maximum drag reduction and the cavity depth for optimum performance are sensitive to the design of the ventilation slots.

Base pressure measurements were made on the back plate of the cavity. A total of 48 pressure tappings were distributed over one half of the back plate. Measurements were obtained for a number of cavity configurations with the model in ground proximity; the plain cavity, the initial vented cavity with square edged slots, the vented cavity with tapered slots on all surfaces and the same case but with the underside slots covered. For the two former configurations, base pressure measurements were only made for the optimum drag cavity and a much deeper cavity, while for the two vented cavities with tapered slots the pressure measurements were obtained for a range of cavity depths. In all cases comparison was made with the base pressures measured on the squareback model without a cavity. The effect of cavity depth on the reduction in drag coefficient relative to the squareback configuration is collated from Figures 5 and 7 for the configurations for which base pressure data was obtained and is shown in Figure 8(a).

The measurement of the base pressures allows the drag component obtained on the cavity backplate to be derived and this is shown in Figure 8(b). The reduction in this backplate drag term considerably exceeds the measured overall drag reduction. This implies that the mechanism by which the drag reduction is obtained is itself a source of drag. This drag component is the 'device drag' as defined by Viswanath (6) and it represents the drag obtained from the internal cavity walls, excluding the backplate, and, in the case of the ventilated cavity, the drag from the slots. An estimate of this component can be determined if some basic assumptions are

made. On the simple Ahmed body the total drag coefficient, C_D, comprises the sum of the component coefficients representing the nose drag, C_{DN}, skin friction, C_{DS}, backplate drag, C_{DB}, and the device drag, C_{DD}. The last two terms comprise the base drag component.

$$C_D = C_{DN} + C_{DS} + C_{DB} + C_{DD}$$

If the forebody drag, C_{DF}, the sum of $C_{DN} + C_{DS}$, can be assumed to be independent of the base conditions, it can be obtained directly from the baseline squareback configuration with no cavity,

$$C_{DF} = (C_D - C_{DB})_{\text{Squareback}}$$

and therefore,

$$C_{DD} = C_D - C_{DB} - C_{DF} = C_D - C_{DB} - (C_D - C_{DB})_{\text{Squareback}}$$

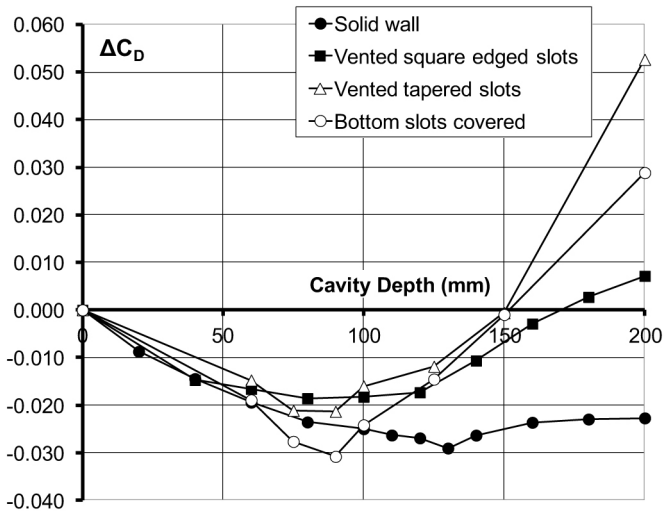

Figure 8(a). Effect of cavity depth on total drag.

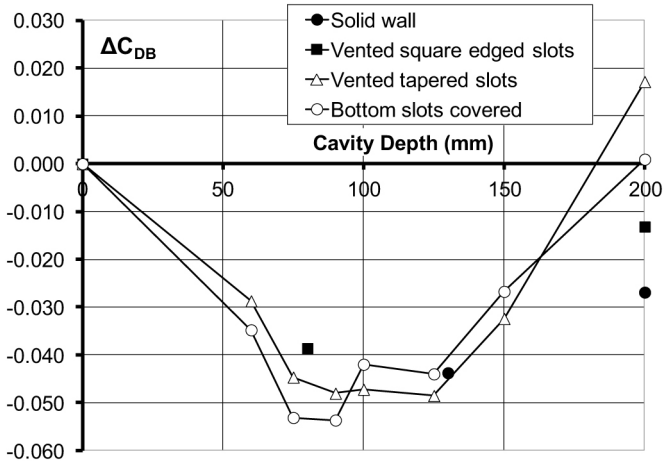

Figure 8(b). Effect of cavity depth on the backplate drag component.

The device drag coefficient term, C_{DD}, is plotted in Figure 9. There is probably some loss of accuracy through the multiple operations to determine the device drag term, but the trends are reasonably clear. For all the vented cavity cases the device drag rises with increasing cavity depth, and ventilation area, to a depth comparable with the minimum drag depth and then levels off. The exception to this trend is shown by the plain cavity where the device drag appears to fall as the cavity depth increases beyond the depth for minimum overall drag. Very limited data is available but the deepest cavity shows a near zero device drag component. The introduction of the ventilation to the cavity increases the device drag component considerably. In magnitude it is comparable to the maximum net drag reduction achieved.

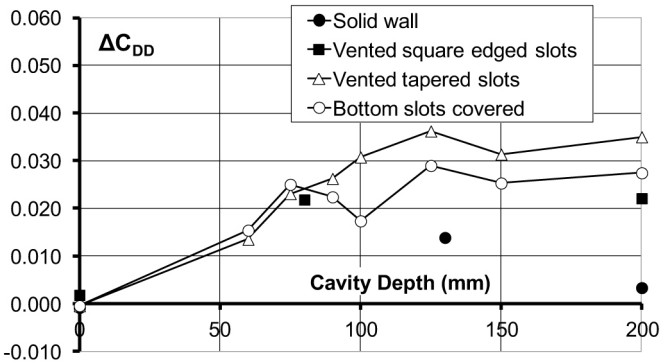

Figure 9. Effect of cavity depth on the 'device drag' component.

PIV was used to visualise the airflow on the model centerline with the body in ground proximity. Results are shown in Figures 10(a) and (b) for the squareback model and for the model with a plain cavity 130mm deep, respectively. The cavity depth represents the optimum drag condition. Figure 11 shows the difference between these two plots in order to highlight the effect of the cavity.

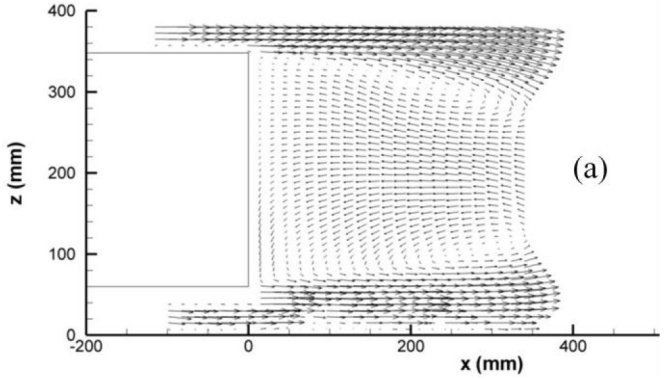

Figure 10. PIV on Centreline (a) Squareback, (b) PlainCavity 130mm deep

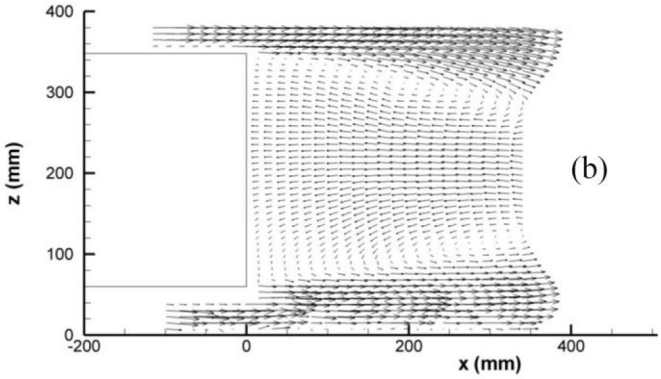

Figure 10 (Cont'd). PIV on Centreline (a) Squareback, (b) PlainCavity 130mm deep

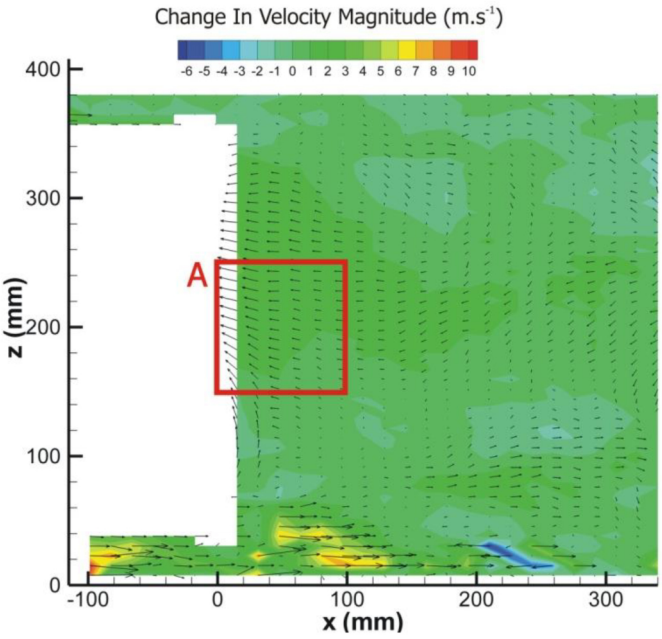

Figure 11. Change in vector field on Centreline between Squareback and PlainCavity 130mm deep.

Figure 12 shows the PIV images for the base cavity incorporating tapered ventilation slots. Figure 12(a) shows the case where all the cavity walls are slotted, while in Figure 12(b) the slots on the underside of the cavity are sealed. Figure 13 highlights the differences between these two plots, showing an impact on the lower separating shear layer, and seems to indicate a downward shift.

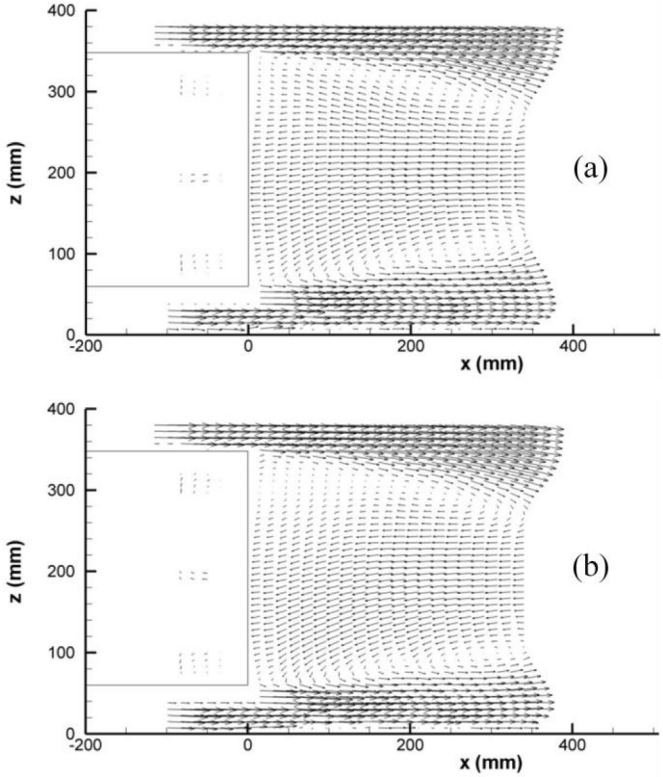

Figure 12. PIV on Centreline. (a) Ventilated Cavity90mm deep, (b) Ventilated Cavity 90mm deep-Underside solid.

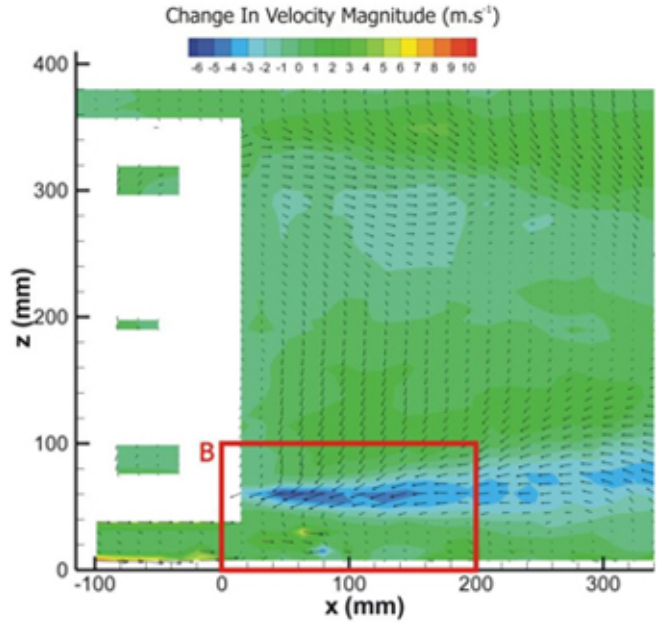

Figure 13. Change in vector field on Centreline when underside slots are closed (Ventilated Cavity90mm deep)

While there are some changes in the flow structure, there are no major modifications to the separating shear layer to indicate why the cavity is effective or why the ventilation

slots reduce the cavity depth for a given reduction in drag. The significant changes are to the base pressure. It is suggested that the base pumping effect of the separating shear layer, which is the primary mechanism creating base pressure, according to Hoerner (17), is less effective because the base surface is more remote from the shear layer 'pump'. Some additional flow measurements have been made along the near wake centerline using a 5-hole pressure probe for a selection of model configurations, as shown in Figure 14. These show the unsteady pressure level as measured at the centre hole of the probe. The intensity of the unsteadiness in the upper separating shear layer from the base is clearly shown. The upper plot represents the squareback configuration, with no cavity, and demonstrates the most unsteady behaviour. The lower plots show that the shear layer unsteadiness is reduced for the plain cavity at optimum depth and reduced further for the vented cavity, also at optimum depth. This could indicate that shear layer unsteadiness is reduced as the overall drag is reduced. Morel, (7), however, has shown that for plain cavities overall drag and turbulence intensity in the shear layer appears to be related, but this is not the case for ventilated cavities. Care should therefore be taken in interpreting this result.

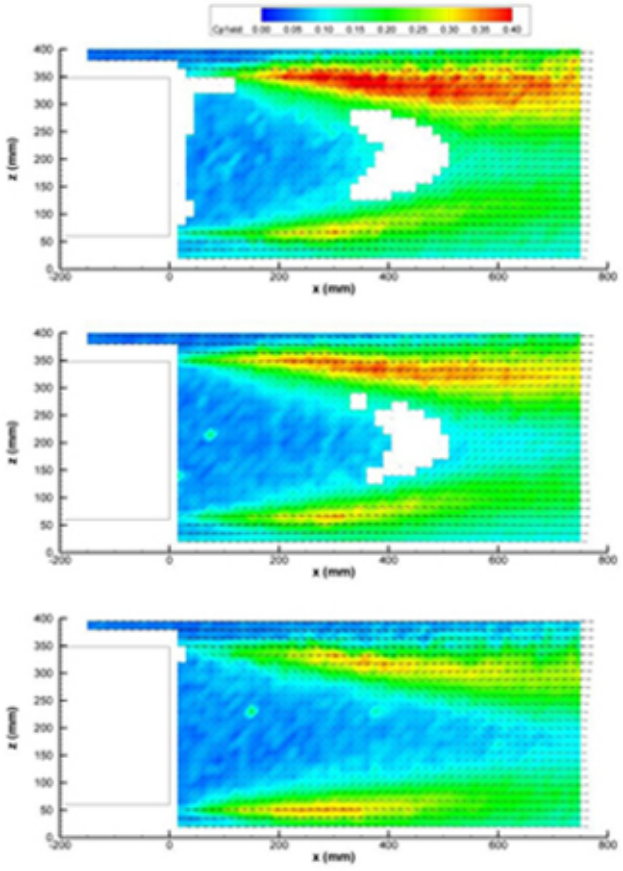

Figure 14. Unsteady Pressure on Wake Centreline (top) Squareback, (middle) PlainCavity 130mm deep, (bottom) Vented cavity (solid underside) 90 mm deep.

It may be instructive to compare the drag reduction obtained in this experiment, using simple models, with earlier wind tunnel tests on real vehicles or more realistic vehicle models. Mason and Beebe, (10), obtained a drag coefficient reduction of $\Delta C_D = -0.030$ on a truck model with a 3-sided plain cavity. The cavity depth was given by $L/D_e = 0.13$. Hucho, (11), reports on a plain cavity fitted to the rear of a VW Camper Van. At a cavity depth of 22% of the vehicle length the drag reduction was 6%, giving an estimated drag reduction of approximately $\Delta C_D = -0.025$. The primary author of this paper, (JH), in an unreported wind tunnel test, applied a plain 3-sided cavity to an SUV, with modifications to the body side and roof trailing edges to produce a squareback configuration. A drag coefficient reduction of $\Delta C_D = -0.012$ was obtained at a cavity depth given by $L/D_e = 0.21$, although no deeper cavities were investigated. A subsequent investigation on an SUV by Irving Brown et al, (12), found insignificant drag benefits. Larger drag reductions have been measured on trucks with angled base plates, forming a combined boat-tail and cavity. Cooper, (1), obtained wind averaged drag coefficient reductions of $\Delta C_D = -0.040$ and $\Delta C_D = -0.060$ for a straight truck and a tractor-trailer respectively, with a boat-tail angle of 15° and cavity depth of $L/D_e = 014$. Browand et al, (2), obtained equivalent drag reductions, (using fuel economy data), of $\Delta C_D = -0.058$ in field tests on a tractor-trailer fitted with angled base plates having a boat-tail angle of 13° and a cavity depth of approximately $L/D_e = 019$. Some additional benefit is apparent from combining a cavity with boat-tailing.

CONCLUSIONS

Wind tunnel tests have been conducted on a simple bluff shape, the Ahmed body, in squareback configuration, to investigate the drag benefits from a rear cavity.

A maximum drag reduction of approximately $\Delta C_D = -0.030$ was obtained in freestream conditions and in ground proximity. The cavity depth, L, for maximum drag reduction was obtained at $L/D_e = 0.37$, where D_e is the effective body diameter, for the body in freestream and at $L/D_e = 0.34$ in ground proximity.

Initial investigation of the effects of ventilating the cavity with slots showed that the maximum drag reduction was reduced, but the cavity depth for minimum drag was also reduced, The drag rise for cavity depths greater than the optimum was significant.

Modification of the slot geometry to reduce the device drag improved the performance of the cavity but a comparable drag reduction to that obtained with the plain cavity was only achieved by sealing the slots on the underside of the cavity. The optimum drag was obtained with a cavity depth given by $L/D_e = 0.27$.

From base pressure measurements the magnitude of the device drag component has been derived and is shown to be significant. It can exceed 10% of the overall drag and is

comparable to the maximum net reduction in the overall drag coefficient achieved.

REFERENCES

1. Cooper, K., "Truck Aerodynamics Reborn - Lessons from the Past," SAE Technical Paper 2003-01-3376, 2003, doi:10.4271/2003-01-3376.
2. Browand, F., Radovich, C., and Boivin, M., "Fuel Savings by Means of Flaps Attached to the Base of a Trailer: Field Test Results," SAE Technical Paper 2005-01-1016, 2005, doi:10.4271/2005-01-1016.
3. Englar, R., "Drag Reduction, Safety Enhancement, and Performance Improvement for Heavy Vehicles and SUVs Using Advanced Pneumatic Aerodynamic Technology," SAE Technical Paper 2003-01-3378, 2003, doi:10.4271/2003-01-3378.
4. Sykes, D.M., The Effect of Low Flow Rate Gas Ejection and Ground Proximity on After Body Pressure Distribution. Road Vehicle Aerodynamics, 1st Symposium The City University, London, November, 1969.
5. Howell, J., Sheppard, A., and Blakemore, A., "Aerodynamic Drag Reduction for a Simple Bluff Body Using Base Bleed," SAE Technical Paper 2003-01-0995, 2003, doi:10.4271/2003-01-0995.
6. Viswanath, P.R., Flow Management Techniques for Base and Afterbody Drag Reduction. Prog. Aerospace Sci., Vol 32, pp79-129, 1996.
7. Morel, T., Effect of Base Cavities on the Aerodynamic Drag of an Axisymmetric Body. Aeronautical Qtly, 30, 400-412, 1979.
8. Duell, E. and George, A., "Measurements in the Unsteady Near Wakes of Ground Vehicle Bodies," SAE Technical Paper 930298, 1993, doi: 10.4271/930298.
9. Duell, E. and George, A., "Experimental Study of a Ground Vehicle Body Unsteady Near Wake," SAE Technical Paper 1999-01-0812, 1999, doi:10.4271/1999-01-0812.
10. Mason, W.T., Beebe, P.S., The Drag Related Flow Field Characteristics of Trucks and Buses. Aerodynamic Drag Mechanisms of Bluff Bodies and Road Vehicles, Ed. Sovran, G., 1976.
11. Hucho, W-H., Aerodynamics of Road Vehicles. 4th Edition, ISBN 0-7680-0029-7, 1998.
12. Irving Brown, Y., Windsor, S., and Gaylard, A., "The Effect of Base Bleed and Rear Cavities on the Drag of an SUV," SAE Technical Paper 2010-01-0512, 2010, doi:10.4271/2010-01-0512.
13. Ahmed, S., Ramm, G., and Faltin, G., "Some Salient Features Of The Time-Averaged Ground Vehicle Wake," SAE Technical Paper 840300, 1984, doi: 10.4271/840300.
14. Sims-Williams, D. and Dominy, R., "The Design of an Open-Jet Wind Tunnel for Model Testing," SAE Technical Paper 2002-01-3340, 2002, doi:10.4271/2002-01-3340.
15. Sims-Williams, D.B., Dominy, R.G., The Design of a New Wind Tunnel for Vehicle Aerodynamics Research. MIRA Vehicle Aerodynamics Conference, Warwick, UK, 2002.
16. Aerodynamic Testing of Road Vehicles in Open Jet Wind Tunnels. SAE SP1465, SAE International, ISBN 0-7680-0443-8, 1999.
17. Hoerner, S. Fluid-Dynamic Drag. Published by the author, 1965.

CONTACT INFORMATION

Jeff Howell
Senior Technical Specialist - Aerodynamics
Tata Motors European Technical Centre
University of Warwick
Coventry CV4 7AL
UK
jeff.howell@tatamotors.com

ACKNOWLEDGMENTS

The research for this paper was funded through the Low Carbon Vehicle Technology Project (LCVTP), a collaborative research project between leading automotive companies and research partners. The project partners included Jaguar Land Rover, Tata Motors European Technical Centre, Ricardo, MIRA Ltd., Zytek, WMG and Coventry University. The project was funded by Advantage West Midlands (AWM) and the European Regional Development Fund (ERDF), and comprised 15 automotive technology development work-streams including Workstream 12 for Aerodynamic drag reduction. The support of the workstream partners and TMETC is acknowledged. Particular thanks go to Geoff le Good for establishing support from different universities and to Hussain Ali of the TMETC Aerodynamics department.

DEFINITIONS/ABBREVIATIONS

A
Frontal area

A_v
Ventilation area

C_D
Drag coefficient

C_{DB}
Cavity backplate drag coefficient

C_{DD}
Device drag coefficient

C_{DF}
Forebody drag coefficient

C_{DN}
Nose drag coefficient

C_{DS}
Surface drag coefficient

D_e
Equivalent diameter

L
Cavity depth

M
Mach number

Re
Reynolds number

x
Distance downstream of trailing edge

z
Height above ground plane

z_0
Ground clearance